ARTICLES

Microtwinning in Template-Synthesized Single-Crystal Metal Nanowires

Jinguo Wang,*,† Mingliang Tian,†,‡ Thomas E. Mallouk,†,§ and Moses H. W. Chan†,‡

Materials Research Institute and The Center for Nanoscale Science (MRSEC), The Pennsylvania State University, University Park, Pennsylvania 16802-6300, Department of Physics, 104 Davey Laboratory, The Pennsylvania State University, University Park, Pennsylvania 16802-6300, and Department of Chemistry, 108 Davey Laboratory, The Pennsylvania State University, University Park, Pennsylvania 16802-6300

Received: April 21, 2003; In Final Form: November 4, 2003

Twinning is one of the most popular planar defects in nanocrystals, and it is frequently observed in face-centered cubic (fcc) structured metallic nanocrystals. In this study, copper, silver, and gold nanowires with diameters of 30−50 nm were prepared by electrochemical deposition in "track-etched" polycarbonate membranes. High-resolution transmission electron microscopy (HRTEM) and electron diffraction were used to study the microstructure of the nanowires. Microtwins were observed to be dependent on growth orientation in the single-crystal metal (copper, silver, and gold) nanowires. In single-crystal nanowires with a [111] growth orientation, both primary (111)[11$\bar{2}$] and secondary ($\bar{1}\bar{1}$1)[112] twins were observed, whereas in the wires with a [11$\bar{2}$] growth orientation, lengthwise twins and stacking faults were the dominant features. No twinning was observed in nanowires that grew along the [100] and [110] directions. The crystallography of the twins was characterized by HRTEM and electron microdiffraction. The twinning mechanism (nucleation and growth) is discussed in relation to a two-dimensional (2D) nucleation and growth mechanism for the single-crystal nanowires.

I. Introduction

Nanoscale one-dimensional (1D) materials have stimulated great interest, because of their importance in basic scientific research and potential technological applications.[1,2] Among various synthetic processes, template synthesis has been proven to be a versatile and simple approach for the preparation of metal nanowires and/or nanotubes.[3] Arrays of nanowires are obtained by filling a porous template that contains a large number of straight cylindrical holes with a narrow size distribution. The method has been used to prepare both nanotubules and nanofibrils composed of conductive polymers, metals, semiconductors, carbon, and other materials.[3−5] The method was first introduced by Possin, who prepared different metallic wires with diameters as small as 40 nm in pores of etched nuclear damage tracks in mica.[6,7] The method was thereafter refined by Willams and Giordano, who obtained silver wires with diameters of <10 nm;[8] using the same modified method, Masden and Goordano studied the electron localization in platinum nanowires.[9] Membranes filled with cobalt, nickel, and iron are magnetic nanocomposites that have strong perpendicular magnetic anisotropy suitable for perpendicular recording.[10−13] Penner and Martin demonstrated the successful synthesis of conducting polymers (pyrrole and polythiophene) from commercial screen membranes, which are polycarbonate foils with pores obtained by etching nuclear damage tracks.[14] Instead of wires, it is also possible to synthesize tubules.[15] In addition, pores have successfully been filled with two different materials that were stacked alternatingly to form multilayers.[11,16−18] Metal (gold, silver, or copper) nanowires are among the most interesting materials for exploration of the fundamental mechanisms of growth and physical properties. Metal nanowires with single-crystal and polycrystalline structures have been synthesized using the template synthetic method.[19−24]

Recently, studies on lead[25] and gold[26] nanowires showed that their physical properties were strongly dependent on their microstructures. Because the scattering of electrons at grain boundaries and other defects will strongly affect the physical properties when lateral dimensions or grain size become comparable to the electron mean free path, it is important to understand the details of defect structure in metal nanowires.

Twinning is one of the most common planar defects in nanocrystals, and it is frequently observed in face-centered cubic (fcc) structured metallic nanocrystals. As a major microstructural characteristic, it is expected to have important effects on the physical (particularly, the electronic and mechanical) properties. Mechanically, twin boundaries can act as obstacles to dislocations, just as the grain boundaries do, and, therefore, have effects on the deformation behavior of nanocrystalline copper.[27,28] Twins have been observed in copper[21] and silver[22] nanowires. However, there have been no systematic studies of twin formation in single-crystal and polycrystalline nanowires. Recently, we have successfully fabricated gold, silver, and copper wires with diameters of 30−300 nm. We found that the textures of nanowires with different diameters can be manipulated from polycrystalline to single crystalline by changing the electrodeposition parameters and by adding surfactants or

* Author to whom correspondence should be addressed. E-mail: jqw11@psu.edu.

† Materials Research Institute and The Center for Nanoscale Science (MRSEC).

‡ Department of Physics.

§ Department of Chemistry.

10.1021/jp035068q CCC: $27.50
Published on Web 12/18/2003

polymers to the plating solutions.[19] Here, we will report a detailed study of the microtwins that are formed in template-grown single-crystal metal nanowires.

II. Experimental Details

The metallic nanowires used in this work were fabricated by electrodepositing metals (gold, silver, and copper) into porous polycarbonate membranes with a nominal pore size of 10 nm, as quoted by the manufacturers. The thickness and pore density of the membranes are 6 μm and 6×10^8 pores/cm^2, respectively. The electrolytes for gold (and silver) depositions are prepared in the following manner: a small amount of gelatin (~2 wt %) was added into 20 mL of commercial Orotemp gold (1025 Ag bath, Technic, Inc.) and then diluted with water to 40 mL. The electrolyte for copper deposition was prepared using a $CuSO_4 \cdot 5H_2O$ aqueous solution (125 g/L) with 1% gelatin (by weight); the pH value was adjusted to 1, using concentrated H_2SO_4. Electrodeposition was performed in a glass tube cell; a platinum wire that was 1 mm in diameter and a saturated calomel electrode (SCE) were used as the counter electrode and the reference electrode, respectively. A thin gold (or silver) film, which was evaporated on one side of the membrane prior to the electrolysis, served as the working cathode, whereas the other side without conducting film faced the plating solution. By controlling the electrodeposition parameters (such as potential, temperature, and the appropriate surfactants or soluble polymers), the microstructures of the nanowires can be manipulated from single-crystal, bamboolike crystalline to polycrystalline structures.[19] It was found that, with the gelatin additive and at 40° C, single-crystal gold nanowires can be obtained with an overpotential (V_{SCE}) between −0.7 V and 0.6 V. Between −0.9 V and −0.7 V, bamboolike crystalline wires resulted, in which the boundaries between the two single-crystal segments are twin boundaries. A more negative potential ($V_{SCE} < -1.0$ V) will produce polycrystalline wires.[19] Similarly, single-crystal silver and copper wires were also fabricated with deposition potentials of $V_{SCE} \approx -0.9$ and −0.1 V, respectively.

The nanowires were harvested by dissolving the polycarbonate membrane in dichloromethane and precipitating material from the solvent by means of a centrifuge. The free-standing nanowires were stored as a suspension in ethyl alcohol. Transmission electron microscopy (TEM) specimens were prepared by placing a drop of the nanowire suspension on a Lacey carbon grid. TEM data were obtained on a Hitachi model HF-2000 field-emission transmission electron microscope that was operated at 200 kV.

III. Results

Figure 1 shows a typical TEM image and X-ray diffraction (XRD) pattern of free-standing single-crystal gold nanowires with a diameter of 40 nm, which is 4 times larger than the nominal pore size of 10 nm that was reported by the membrane manufacturer. Diffraction and HRTEM analyses showed that most of the wires grew with a [111] orientation, whereas some of the wires grow along the [11$\bar{2}$], [100], and [110] directions.[19] The HRTEM image in Figure 2a shows a gold tip growing along the [111] direction. The nanowire is aligned with the beam perpendicular to the [111] growth axis and parallel to the [1$\bar{1}$0] zone axis. A twin boundary across the wire is clearly present; the end portion of the tip is a twin from the matrix. The twinning elements are given in Figure 2b. Apparently, the twin system is (111)[11$\bar{2}$], which is the primary twinning system in the fcc gold nanowires. Another twin, the so-called "secondary twin", is also frequently observed in single-crystal nanowires that are

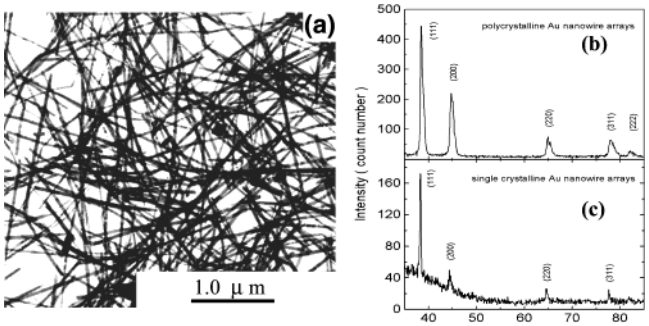

Figure 1. Typical (a) TEM image and (b) X-ray diffraction (XRD) pattern of free-standing single-crystal gold nanowires with a diameter of 40 nm.

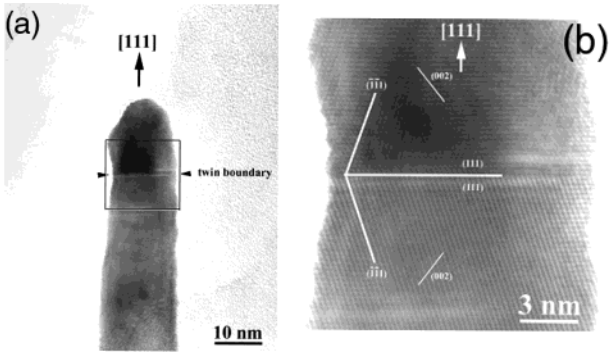

Figure 2. (a) HRTEM image of a growing gold nanowire tip with a twin boundary along the [111] direction; (b) HRTEM image of the twinning elements.

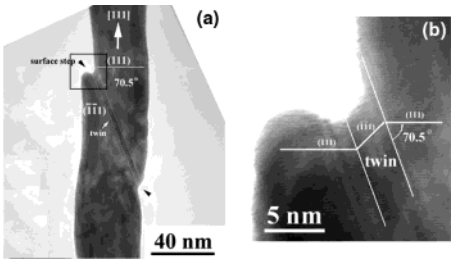

Figure 3. (a) HRTEM image of a ($\bar{1}\bar{1}$1)[112] twin in a 40-nm-diameter gold nanowire; (b) HRTEM image of the local enlargement of the twin area.

growing along the [111] direction. An example is shown in Figure 3, where the twining plane is ($\bar{1}\bar{1}$1) and the twinning orientation is [112]. The twinning plane ($\bar{1}$1$\bar{1}$) has an angle of 70.5° from the (111) growth orientation. It should also be noted that, on both ends of the twin, at the surface of the nanowire, two ledges exist, which are very important in regard to understanding twin formation. Figure 4 shows another single-crystal gold nanowire with a [111] growth orientation. Both a primary (111)[11$\bar{2}$] twin and a secondary ($\bar{1}\bar{1}$1)[112] twin are observed in the wire, and they intersect at the point indicated by the black arrow in the figure. In this case, the primary twin is thinner than the secondary twin and was twinned by the secondary twin, altering the orientation in the secondary twin ($[111]_T = [115]_M$). Figure 5 shows a multiply twinned copper nanowire with a [111] growth orientation. The wire is wrapped in a copper oxide shell. Several primary (111)[11$\bar{2}$] twins and a secondary ($\bar{1}$1$\bar{1}$)[112] twin are apparent. Also, in the growing end of the wire, which is a secondary twin of the upper portion, there are two primary twins along the $[111]_T$ or $[115]_M$ orientation.

In nanowires with a growth orientation along the [11$\bar{2}$] direction, lengthwise (111)[11$\bar{2}$] twins and stacking faults are

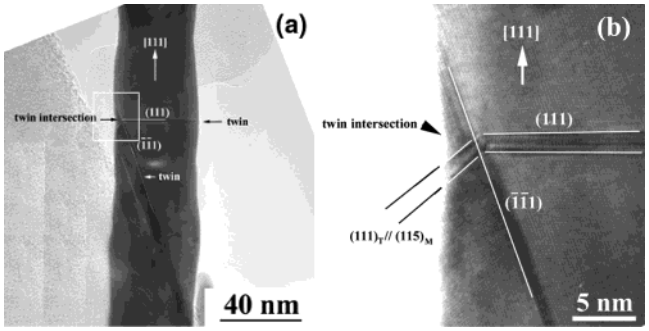

Figure 4. (a) HRTEM image of the twin intersection in a gold single-crystal nanowire with [$\bar{1}11$] growth orientation; a primary (111)[$11\bar{2}$] twin, and a secondary ($\bar{1}\bar{1}1$)[112] twin intersect at the point indicated by the left arrow. A local enlargement of the intersection area is shown in panel b.

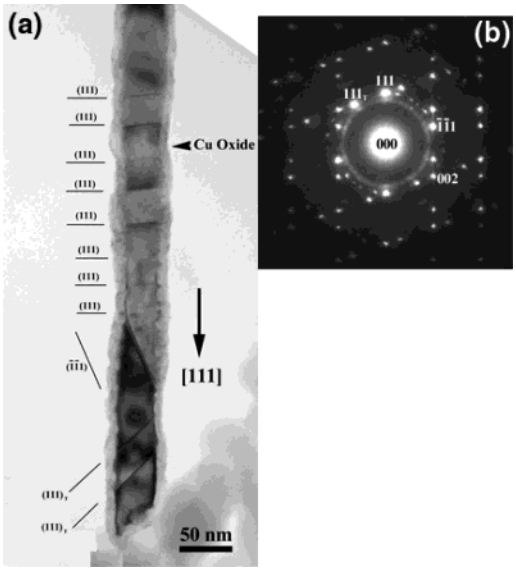

Figure 5. (a) HRTEM image of twins in a copper single-crystal nanowire with a growth orientation along the [111] direction; (b) the corresponding diffraction pattern.

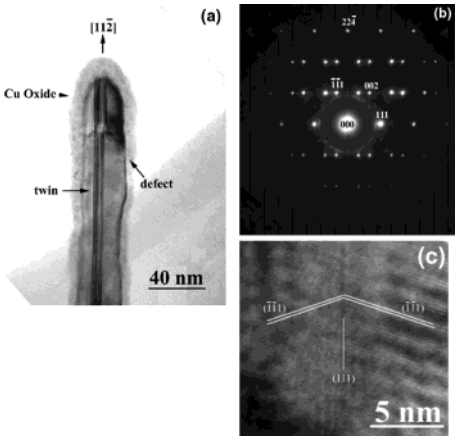

Figure 6. (a) HRTEM image of the lengthwise (111)[$11\bar{2}$] twins in a single-crystal copper wire; the corresponding electron diffraction pattern and a high-resolution image along the [110] direction are shown in panels b and c, respectively.

the dominant defects. An example of this type of lengthwise (111)[$11\bar{2}$] twin in a single-crystal copper wire is shown in Figure 6a. The corresponding electron diffraction pattern and the high-resolution image along the [$1\bar{1}0$] direction are shown in panels b and c, respectively, in Figure 6. The pattern is characteristic of a fcc material that is twinning on {111}-type

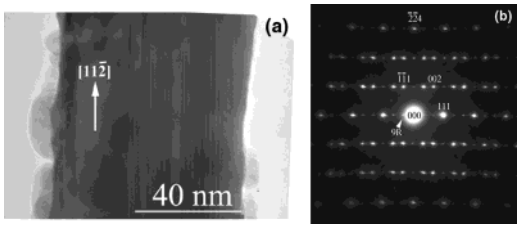

Figure 7. (a) Stacking faults and twins in a silver single-crystal nanowire with [$11\bar{2}$] growth orientation; (b) corresponding electron diffraction pattern.

planes and consists of overlapping patterns from the matrix and the twins (as indexed). The growth axis of the nanowire is along the [$11\bar{2}$] direction, as demonstrated by the diffraction pattern. Streaking along the [111]* reciprocal lattice direction results primarily from the limited number of scatterers in this direction in the thin wire. The diffraction ring in the center of the pattern may result from the oxide shell. The formation of copper oxides was also reported by Gao et al.,[29] who found that lower overpotentials are necessary to avoid the formation of copper oxides.

A HRTEM image of a single-crystal silver nanowire with a [$11\bar{2}$] growth orientation is shown in Figure 7a. Along with the lengthwise microtwins, there are many stacking faults on the (111) plane. The corresponding electron diffraction pattern is shown in Figure 7b. Extra diffraction spots are apparent in the pattern, compared to the diffraction pattern in Figure 6b. The extra spots are located at a distance equal to one-third of the spacing of the [111]* spots in reciprocal space. This is a characteristic 9R structure, which is commonly observed in metals under phase transformation or deformation.[30] We did not observe the 9R structure in the copper or gold nanowires, which may be because silver has a lower stacking fault energy (19 ± 3 erg/cm^2) compared to that of gold (47 ± 7 erg/cm^2) and copper (62 ± 9 erg/cm^2).[31]

Panels a and b in Figure 8 show gold nanowires that have grown along the [100] and [110] directions, respectively, and the corresponding electron diffraction patterns are shown next to the TEM images in each panel. The wire surfaces have a rippled shape; however, no twins or stacking faults were observed in the wires with these orientations. The same situation was found in copper and silver nanowires with [100] and [110] orientations, which is consistent with similar observations made with silicon nanowires.[32]

IV. Discussion

We have developed a method for manipulating nanowire microstructures from single crystal to polycrystalline by controlling the electrodeposition parameters and the addition of surfactants and soluble polymers.[19] The single-crystal nanowires follow a two-dimensional (2D) nucleation and growth mechanism, whereas the polycrystalline nanowires have a three-dimensional (3D) nucleation and growth mechanism.[19] Here, we will briefly discuss the twinning mechanism in single-crystal nanowires, on the basis of the 2D nucleation and growth mechanism.

In the 2D nucleation and growth model, the nucleation and growth of the twin occur at the liquid/solid interface by a terrace−ledge−kink mechanism on low-index crystallographic planes (see Figure 9a), such as {111} and {002}. Figure 9b shows a schematic model that was proposed by Hinton et al.[18] for the formation of twins or stacking faults. A large adsorbed foreign molecule, such as a polymeric additive in the electroplating bath, would force an advancing growth step to reverse

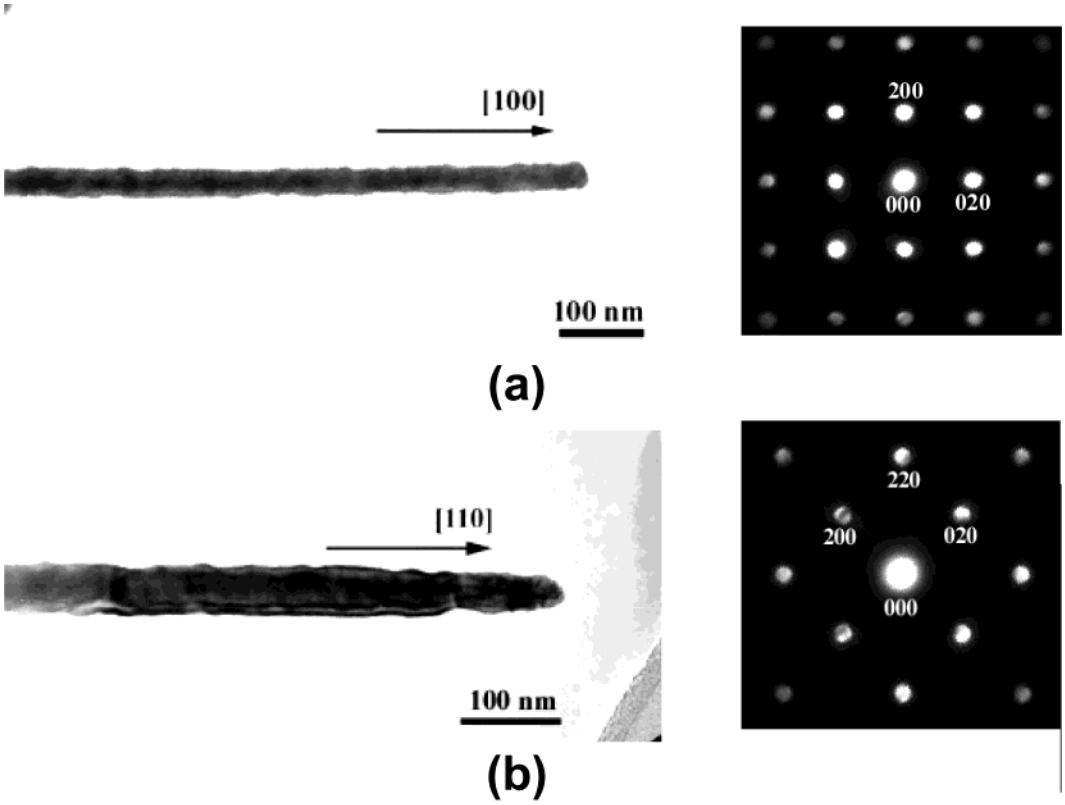

Figure 8. TEM images (left) and the corresponding electron diffraction patterns (right) of gold nanowires grown along the (a) [100] and (b) [110] directions, respectively.

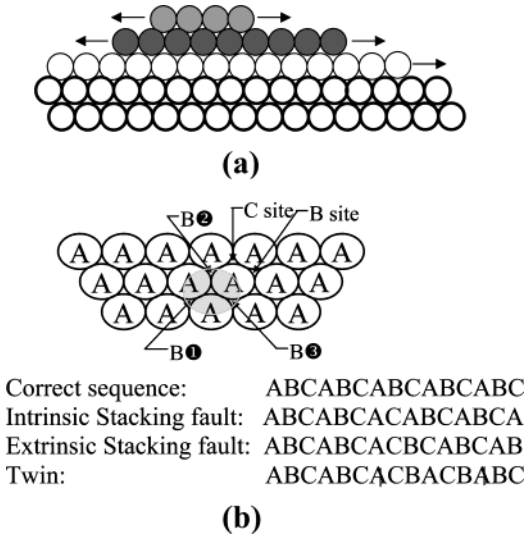

Figure 9. (a) Schematic drawing of the two-dimensional (2D) nucleation and growth model; (b) schematic model for the formation of twins or stacking faults proposed by Hinton et al.[18]

its stacking sequence and, hence, create a twin. A (111) plane in an fcc structure is shown in Figure 9b. An adatom deposited on such a plane will preferentially seek "B-sites", which would continue the structure in the correct stacking sequence. Additive molecules will have no such preference. In Figure 9b, a molecule somewhat larger than an adatom is shown adsorbed at a "C-site" in the next layer. This will force the adatom onto C-sites, creating a fault; hence, the twins are in-grown. Recent work by Zhou and Wadley[33] shows that the binding energy difference for adatoms that occupy either B-sites or C-sites is so small that adatoms can occupy both sites with almost equal probability. This results in the extensive nucleation of twin domain during copper growth in the ⟨111⟩ directions. This means that invoking the adsorption of large foreign molecules is not necessary, because the twin nucleation and growth are intrinsic characteristics of the electrodeposition. No faulted lattice sites are available during growth in the [100] and [110] directions; hence, no twin nucleation was observed. Here, we must emphasize the surface effect of the template pore on the twin nucleation and growth. The surface of the pore is not atomically flat; therefore, the irregularity will act as a larger molecule to force the adatoms onto fault sites, causing twin nucleation. Especially, when the irregularity is directional, it will create a step on the surface of the nanowire that will favor the formation of secondary twins (see Figure 4). Note that secondary twins are not commonly observed in film deposition,[33] in which case there is no surface effect. A possible explanation for the lengthwise (111)[11$\bar{2}$] twin in nanowires with [11$\bar{2}$] orientation could be the growth of the existing nuclei that contain the twins and stacking faults. The nuclei may result from the coalesce of several clusters that possess different ⟨111⟩ orientations, because the (111) planes are low-energy planes in which the twin growth may be favored.

Finally, we also emphasize that these microtwins (boundaries) might have very important roles in the electronic properties of single-crystal nanowires. This is because the scattering of electrons by grain boundaries and surfaces is similar when the wire dimensions are comparable with the grain size or the electron mean free path.[34] For single-crystal wires, it is still unclear whether the twin boundaries act as grain boundaries or as surfaces; further studies on the transport properties of these twinned wires are needed to answer this question.

V. Conclusions

High-resolution transmission electron microscopy (HRTEM) and electron diffraction have been used to study the microstructure and twinning of template-grown metal nanowires. Microtwins were found to be dependent on the growth orienta-

tion in single-crystal copper, silver, and gold nanowires. In single-crystal nanowires with a [111] growth direction, both primary (111)[11$\bar{2}$] and secondary ($\bar{1}\bar{1}$1)[112] twinnings were observed. In contrast, in wires with a [11$\bar{2}$] growth orientation, lengthwise twins and stacking faults were the dominant features. No twinning was observed in nanowires grown along the [100] or [110] directions. In the two-dimensional (2D) nucleation and growth model, the nucleation and growth of the twin occurs at the liquid/solid interface via a terrace−ledge−kink mechanism on low-index crystallographic planes. The formation of twins comes from the possibly faulted lattice sites in the [111] growth orientation. The small binding energy difference for adatoms that occupy the normal lattice site and the fault site results in the extensive nucleation of twin domains. No faulted lattice sites were available during growth in the [100] and [110] directions; hence, no twin nucleation was observed.

Acknowledgment. This work is supported by a Seed Grant provided by the Penn State Materials Research Institute and the Penn State MRSEC (under NSF Grant Nos. DMR 0080019 and DMR 0213623). The TEM experiments were conducted at TEM facility at the Materials Research Institute.

References and Notes

(1) Appell, D. *Nature* **2002**, *419*, 553.
(2) Cobden, D. H. *Nature* **2001**, *409*, 32.
(3) Martin, C. R. *Science* **1994**, *266*, 1961.
(4) Martin, C. R. *Chem. Mater.* **1996**, *8*, 1739.
(5) Huczko, A. *Appl. Phys. A* **2000**, *70*, 365.
(6) Possin, C. E. *Physica* **1971**, *55*, 339.
(7) Possin, C. E. *Rev. Sci. Instrum.* **1970**, *41*, 772.
(8) Williams, W. D.; Giordano, N. *Rev. Sci. Instrum.* **1984**, *55*, 410.
(9) Madsen, J. T.; Giordano, N. *Phys. Rev. B* **1985**, *31*, 6395.
(10) Whitney, T. M.; Jiang, J. S.; Searson, P. C.; Chien, C. L. *Science* **1993**, *261*, 1316.
(11) Piraux, L.; George, J. M.; Despres, J. F.; Leroy, C.; Ferain, E.; Legras, R.; Ounadjela, K.; Fert, A. *Appl. Phys. Lett.* **1994**, *65*, 2484.
(12) Liu, K.; Nagodawithana, K.; Searson, P. C.; Chien, C. L. *Phys. Rev. B* **1995**, *51*, 7381.
(13) Sellmyer, D. J.; Zheng, M.; Skomski, R. *J. Phys.: Condens. Matter* **2001**, *13*, R443.
(14) Penner, R. M.; Martin, C. R. *J. Electrochem. Soc.* **1986**, *133*, 2206.
(15) Brumlik, C. J.; Menon, V. P.; Martin, C. R. *J. Mater. Res.* **1994**, *9*, 1174.
(16) Blondel, A.; Meier, J. P.; Doudin, B.; Ansermet, J.-P. *Appl. Phys. Lett.* **1994**, *65*, 3019.
(17) Gudiksen, M. S.; Lauhon, L. J.; Wang, J.; Smith, D. C.; Lieber, C. M. *Nature* **2002**, *415*, 617.
(18) Wu, Y.; Fan, R.; Yang, P. *Nano Lett.* **2002**, *2*, 83.
(19) Tian, M. L.; Wang, J. G.; Kurtz, J.; Mallouk, T. E.; Chan, M. H. W. *Nano Lett.* **2003**, *3*, 919.
(20) Gao, T.; Meng, G. W.; Zhang, J.; Wang, Y. W.; Liang, C. H.; Fan, J. C.; Zhang, L. D. *Appl. Phys. A* **2001**, *73*, 251.
(21) Molares, M. E. T.; Van Buschmann, D. D.; Neumann, R.; Scholz, R.; Schuchert, I. U.; Vetter, J. *Adv. Mater.* **2001**, *13*, 62.
(22) Sauer, G.; Brehm, G.; Schneider, S.; Nielsch, K.; Wehrspohn, R. B.; Choi, J.; Hofmeister, H.; Gösele, U. *J. Appl. Phys.* **2002**, *91*, 3243.
(23) Barbic, M.; Mock, J. J.; Smith, D. R.; Schultz, S. *J. Appl. Phys.* **2002**, *91*, 9341.
(24) Zhang, J.; Wang, X.; Peng, X.; Zhang, L. *Appl. Phys. A* **2002**, *75*, 485.
(25) Yi, G.; Schwarzacher, W. *Appl. Phys. Lett.* **1999**, *74*, 1746.
(26) Bietsch, A.; Michel, B. *Appl. Phys. Lett.* **2002**, *80*, 3346.
(27) Merz, M. D.; Dahlgren, S. D. *J. Appl. Phys.* **1975**, *46*, 3235.
(28) Youngdahl, C. J.; Weertman, J. R.; Hugo, R. C.; Kung, H. H. *Scr. Mater.* **2001**, *44*, 1475.
(29) Gao, T.; Meng, G.; Wang, Y.; Sun, S.; Zhang, L. *J. Phys.: Condens. Matter* **2002**, *14*, 355.
(30) Othen, P. J.; Jenkins, M. L.; Smith, G. D. W. *Philos. Mag. A* **1994**, *70*, 1.
(31) Humble, P.; Forwood, C. T. *Phys. Status Solidi* **1968**, *29*, 99.
(32) Carim, A. H.; Lew, K.-K.; Redwing, J. M. *Adv. Mater.* **2001**, *13*, 1489.
(33) Zhou, X. W.; Wadley, H. N. G. *Acta Mater.* **1999**, *47*, 1063.
(34) Durkan, C.; Welland, M. E. *Phys. Rev. B* **2000**, *61*, 14215.